An evolving autoimmune microenvironment regulates the quality of effector T cell restimulation and function

Rachel S. Friedman[a,b,1], Robin S. Lindsay[a,b], Jason K. Lilly[a,b], Vinh Nguyen[c], Caitlin M. Sorensen[d], Jordan Jacobelli[a,b], and Matthew F. Krummel[d]

[a]Department of Biomedical Research, National Jewish Health, Denver, CO 80206; [b]Department of Immunology, University of Colorado Denver, Aurora, CO 80045; and Departments of [c]Surgery and [d]Pathology, University of California, San Francisco, CA 94143.

Edited by John W. Kappler, Howard Hughes Medical Institute, National Jewish Health, Denver, CO, and approved May 20, 2014 (received for review December 2, 2013)

Defining the processes of autoimmune attack of tissues is important for inhibiting continued tissue destruction. In type 1 diabetes, it is not known how cytotoxic effector T cell responses evolve over time in the pancreatic islets targeted for destruction. We used two-photon microscopy of live, intact, individual islets to investigate how progression of islet infiltration altered the behavior of infiltrating islet-specific CD8$^+$ T cells. During early-islet infiltration, T-cell interactions with CD11c$^+$ antigen-presenting cells (APCs) were stable and real-time imaging of T cell receptor (TCR) clustering provided evidence of TCR recognition in these stable contacts. Early T cell–APC encounters supported production of IFN-γ by T effectors, and T cells at this stage also killed islet APCs. At later stages of infiltration, T-cell motility accelerated, and cytokine production was lost despite the presence of higher numbers of infiltrating APCs that were able to trigger T-cell signaling in vitro. Using timed introduction of effector T cells, we demonstrate that elements of the autoimmune-tissue microenvironment control the dynamics of autoantigen recognition by T cells and their resulting pathogenic effector functions.

autoimmunity | T-lymphocyte reactivation | 2-photon microscopy

Little is known about the maintenance of autoreactive effector T cell activation within peripheral tissues such as the pancreatic islets. Until recently, peripheral tissues were frequently viewed as sites of predetermined T cell effector function that do not require T-cell restimulation by local professional antigen-presenting cells (APCs). Recently, focus has been placed on the role of APCs in T-cell restimulation in peripheral tissues. In viral infection and vaccination models, dendritic cells (DCs) in peripheral tissues are required to induce T cell effector cytokine production and proliferation (1–3). Additionally, in a model of multiple sclerosis, T-cell restimulation by peripheral-tissue APCs promoted effector-cytokine production and infiltration into the central nervous system (4). In models of type 1 diabetes (T1D), it has been suggested that increased T cell effector functions are acquired in the islets (5) and that T-cell restimulation by DCs is required for CD4 T-cell entry into the islets (6).

In models of T1D, autoreactive T cells are initially activated by DCs in the draining pancreatic lymph node (PLN) (7–9) and can then home to the islets. Once islet infiltration is established, the disease can sustain itself within the islets and progresses following PLN or spleen excision (7). Systemic depletion of CD11c$^+$ cells either promotes or prevents disease depending on when during disease progression the depletion is performed (10), raising questions about whether the role of CD11c$^+$ cells varies depending upon the site and timing of antigen presentation.

We and others have shown that, in the pancreatic islets, tissue resident CD11c$^+$ APCs are present in the steady state (11–13) and additional CD11c$^+$ APCs are recruited upon islet infiltration (11). Here, we sought to understand how these APCs modulate the effector state of islet-infiltrating T cells through antigenic restimulation over the course of islet infiltration. We identified distinct phases of T-cell restimulation by analyzing islets at various stages of islet infiltration. Early infiltration was defined by prolonged restimulating T-cell interactions with islet APCs, which were characterized by classical synapses that induced T cells to secrete cytokines and endowed them with the ability to kill their cognate APC. However, heavily infiltrated, late-stage islets lacked sustained restimulating T cell–APC interactions, an effect that we traced to changes in the islet environment.

Results

T-Cell Motility in the Islets Is Increased with Severity of Islet Infiltration. To determine how restimulation of islet-infiltrating T cells at the disease site influences T-cell pathogenicity, we used the RIP-mOva tissue-specific autoimmune disease model. In this model, membrane-bound ovalbumin (ova) is expressed under the rat insulin promoter (14). Adoptive transfer of large numbers of ova-specific OT-I CD8 T cells (5-10 × 10^6 per mouse) results in islet destruction and overt diabetes although, if mice survive, tolerance is reestablished by autoreactive T-cell deletion (15). In our colony, islet infiltration begins approximately 4 d after T-cell transfer, with 30% of recipients developing diabetes 5–14 d after T-cell transfer.

Red fluorescent OT-I.CD2-dsRed T cells (16) were transferred into RIP-mOva recipients with yellow CD11c$^+$ cells (17) (RIP-mOva.CD11c-YFP). Islets were isolated by collagenase digestion of the pancreas, immobilized in low melting temperature agarose, and visualized by two-photon (2P) microscopy. As in human type 1 diabetes, infiltration of the islets was asynchronous, with uninfiltrated-to-destroyed islets residing in the same pancreas. Thus, we categorized the severity of individual islet infiltration volumetrically. In light, mid, and heavy infiltration, T cells occupied <4%, 4–13%, or >13% of the islet volume, respectively (Fig. S1 *A* and *B*). Day 4 post–T-cell transfer included primarily light and uninfiltrated islets whereas day 7 included primarily mid to heavy infiltrated islets (Fig. S1*C*). Islets analyzed were selected based on the ability of individual T

Significance

Autoimmunity is self-perpetuating within the islets at the time of type 1 diabetes diagnosis. However, little is known about how pathogenic effector T cell functions are stimulated within the islets. Here, we show that the infiltration state of the islet affects T cell interactions with antigen-presenting cells and corresponding T cell effector cytokine production within the islets. This work identifies a restimulation event that is modified by the local islet environment as a critical step in the expression of T cell effector functions and autoimmune tissue destruction.

Author contributions: R.S.F. and M.F.K. designed research; R.S.F., R.S.L., J.K.L., V.N., C.M.S., and J.J. performed research; R.S.F. and R.S.L. analyzed the data; and R.S.F. and M.F.K. wrote the paper.

The authors declare no conflict of interest.

This article is a PNAS Direct Submission.

[1]To whom correspondence should be addressed. E-mail: friedmanr@njhealth.org.

This article contains supporting information online at www.pnas.org/lookup/suppl/doi:10.1073/pnas.1322193111/-/DCSupplemental.

cells to be tracked. As a result, islets with dense foci of infiltration and uninfiltrated islets are not represented.

To determine whether islet-infiltrating T cells were likely to be engaging in prolonged interactions with APCs or targets, their motility was analyzed in isolated islets. To allow tracking of individual cells in mid and heavy infiltrated islets, 10% fluorescent OT-I.CD2-dsRed T cells (red) and 90% unlabeled OT-I T cells were cotransferred into RIP-mOva recipients (Fig. 1*A* and Movie S1). After 4–7 d, islets were imaged by 2P microscopy, and the fluorescent cells were analyzed. Representative tracks from 10 min of T-cell tracking showed reduced T-cell motility in islets with light infiltration compared with islets with mid or heavy infiltration (Fig. 1 *A* and *B* and Movie S1). This change in T-cell motility was confirmed by analysis of the mean squared displacement (MSD) over time (Fig. 1*C*), which is a measure of the ability of a T cell to move away from its point of origin. The MSD showed that T cells in islets with light infiltration had significantly less displacement than T cells in islets with mid or heavy infiltration (Fig. 1*C*). Analyses of average T-cell crawling speed (Fig. 1*D*) and T-cell arrest coefficient (Fig. 1*E*) also supported the conclusion that T cells in the light phase of islet infiltration were arrested. The arrest coefficient is the percentage of time that T cells crawled ≤2 μm/min. In islets on day 4 post–T-cell transfer, T cells showed little crawling and increased arrest whereas, by days 6 and 7, the T cells in the islets had achieved an apparent maximal motility rate (Fig. 1*D*). Together, these data show that T cells arrested motility in lightly infiltrated islets, possibly due to antigenic signaling, but gained motility with more extensive islet infiltration.

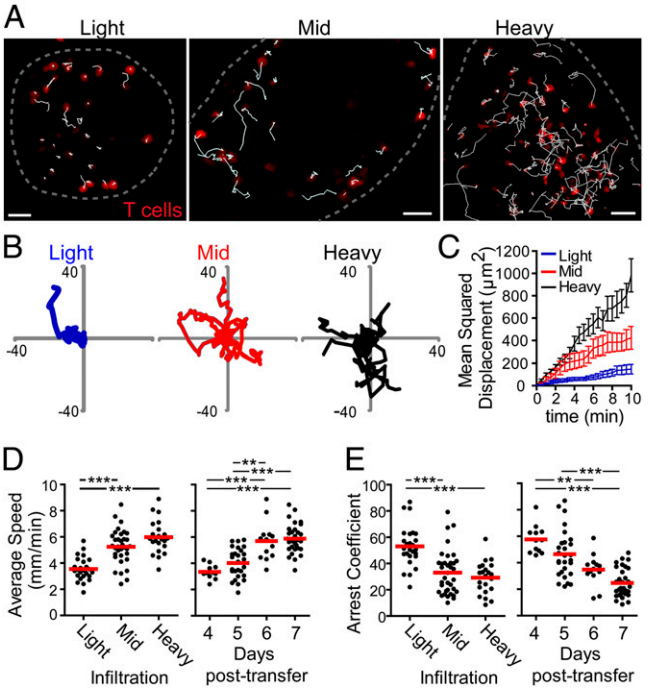

Fig. 1. T cells arrest during early infiltration and regain motility with increased infiltration. CD2-dsRed.OT-I $CD8^+$ T cells or 10% CD2-dsRed.OT-I $CD8^+$ T cells plus 90% OT-I $CD8^+$ T cells were transferred into RIP-mOva or RIP-mOva.CD11c-YFP recipient mice. Islets were isolated 4–7 d following T-cell transfer, immobilized in low-melting agarose, and imaged by time-lapse two-photon microscopy. (*A*) Representative maximum intensity projection images of T-cell (red) motility in islets with light, mid, and heavy T-cell infiltration. All infiltrating OT-I T cells are visualized in the islet with light infiltration whereas only 10% of infiltrating OT-I T cells are visualized in the islets with mid and heavy infiltration. White tracks show the path of T-cell motility over 10 min. The dashed gray line indicates the islet border. (Scale bars: 30 μm.) (*B*) Ten randomly selected T-cell tracks from the islets shown in *A*. Scale shown in μm. (*C*) Mean squared displacement of T cells over 10 min time. Analysis includes all cells tracked in *A*. Error bars = SEM. (*D* and *E*) Quantification of T-cell motility. Each dot represents the average of all tracked T cells in one islet, and the red bar represents the mean of all islets. Data were combined from 82 islets in 13 experiments. Statistical analyses were done using a 1-way ANOVA Kruskal–Wallis test with Dunn's Multiple Comparison Test. $*P < 0.05$, $**P < 0.001$, $***P < 0.0001$. (*D*) Average speed of T-cell crawling in infiltrated islets. (*E*) Arrest coefficient of T cells in infiltrated islets.

T Cells Arrest on $CD11c^+$ Cells During Early-Islet Infiltration. Because our data showed T-cell arrest at early stages of islet infiltration, we sought to determine whether this arrest was due to interactions with $CD11c^+$ APCs. To do so, we quantified T cell–$CD11c^+$ cell interactions. In islets with light infiltration, many T cells that were in close proximity to a $CD11c^+$ cell had sustained interactions with that $CD11c^+$ cell for ≥10 min [Fig. 2*A* (filled arrows) and *B*–*E* and Movie S2], but T cells also arrested without contacting $CD11c^+$ cells (Fig. 2*A*, open arrows and Movie S2). T cells that arrested without contacting $CD11c^+$ cells likely represent interactions with beta cells (18), which were not visualized in our experiments. In contrast, in islets with mid and heavy infiltration, T cells frequently contacted $CD11c^+$ cells (Movie S3 and Fig. 2*B*), likely due to the increased density of both cell types; however, few of these contacts were sustained (Fig. 2 *C*–*E* and Movie S3). Overall, the T cells in islets with mid and heavy infiltration showed little stopping or sustained T cell–APC interactions. These data demonstrate that increased T-cell arrest in lightly infiltrated islets is associated with sustained T cell–CD11c+ APC interactions. In contrast, motile contacts dominated in mid and heavy infiltrates.

PD-1–PD-L1 Interactions Do Not Regulate Changes in T-Cell Motility with Heavy Islet Infiltration. We next sought to determine whether checkpoint receptors or regulatory T cells were likely to be influencing the change in T-cell motility and APC interactions as islet infiltration progressed. To do so, we first stained the islet-infiltrating T cells for FoxP3, PD-1, LAG-3, and CTLA-4. We found a reduction in the percentage of $FoxP3^+$ T cells as islet infiltration progressed (Fig. S2*A*), making it unlikely that the changes in T-cell motility and interactions were due to the effects of regulatory T cells. Expression of PD-1, LAG-3, or CTLA-4 on the islet-specific OT-I T cells did not change over the course of islet infiltration (Fig. S2*B*). Although expression of the checkpoint receptors did not change with islet infiltration, it is possible that ligand expression for these receptors was modulated. Our previous data showed that MHC class II, the ligand for LAG-3, is always highly expressed on $CD11c^+$ APCs in the islets (11). We had also analyzed the expression of CTLA-4 ligands, and, whereas CD80 is modulated with islet infiltration, CD86 is always highly expressed on $CD11c^+$ APCs in the islets (11). The lack of modulation of LAG-3 and CTLA-4 and their ligands suggests that these receptors are unlikely to be mediating changes in T-cell motility and interactions.

We analyzed the expression of the PD-1 ligand PD-L1 on the $CD11c^+$ APCs and beta cells and found that PD-L1 expression was modulated with islet infiltration (Fig. S3*A*). As a result, we used an anti–PD-1 antibody to block PD-1 interactions with its ligands or an isotype control and analyzed T-cell motility on day 7 following T-cell transfer. Blockade of PD-1 did not prevent the acceleration of T-cell motility or reduction in T-cell arrest at late stages of islet infiltration (Fig. S3*B*).

Islet APCs from Early- and Late-Islet Infiltration Present Islet Antigen and Support T-Cell Interactions and Signaling. Because T-cell arrest and sustained T cell–$CD11c^+$ cell interactions varied with islet infiltration, we wanted to test whether the $CD11c^+$ APCs from early- and late-islet infiltration were equivalently able to present islet antigen and support T-cell signaling. We sorted $CD11c^+$ MHC-II^{hi} APCs from islets at early (day 4.5) and late (day 7) time points of infiltration and incubated the sorted APCs with in vitro-activated OT-I T cells labeled with the calcium-sensitive dye Fura-2AM. As a readout of antigen presentation, T-cell

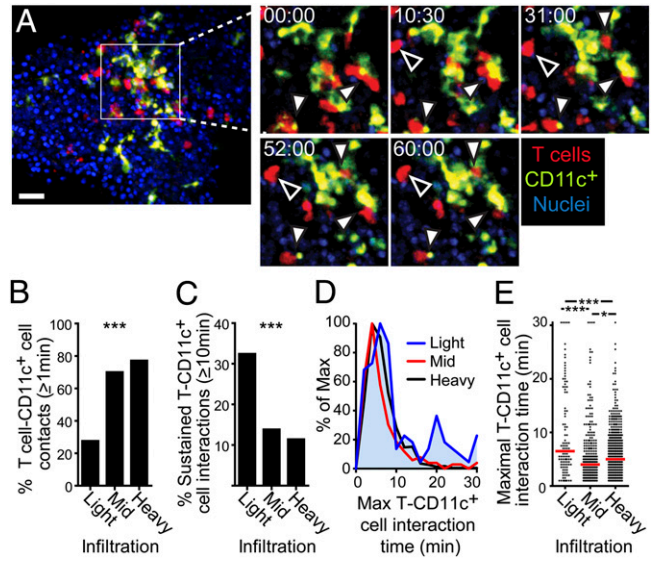

Fig. 2. T cell–APC interactions convert from sustain to transient with increased infiltration. Isolated islets were imaged by time-lapse two-photon microscopy as described for Fig. 1. $*P < 0.05$, $**P < 0.001$, $***P < 0.0001$. (*A*) Representative time-lapse imaging of sustained T-cell interactions in a lightly infiltrated islet. Filled arrowheads indicate sustained interactions of a T cell with a CD11c$^+$ cell, and open arrowheads indicate sustained interactions of a T cell with an unlabeled cell. (Scale bar: 30 μm.) Time-lapse area shown represents 90 μm (x) × 90 μm (y) × 15 μm (z). Time stamp, min:sec. (*B–E*) Quantification of T cell–CD11c+ cell interactions. Data were combined from nine experiments. (*B*) Percentage of T cells that contacted a CD11c$^+$ cells for at least 1 min. (*C*) Percentage of T cells that maintain T cell–CD11c$^+$ cell interactions for at least 10 min. (*B* and *C*) Statistical analyses were done using a Chi Square Test. (*D* and *E*) Duration of the longest T cell–CD11c+ cell interaction per interacting T cell. (*E*) Each dot represents one T cell, and the red bar represents the median. Statistical analyses were done using a 1-way ANOVA Kruskal–Wallis test with Dunn's Multiple Comparison Test.

calcium flux was analyzed during T cell–APC interactions using widefield fluorescence microscopy. Antigen-pulsed CD11c$^+$ MHC-II^{hi} APCs sorted from the spleen were used as a positive control (Fig. 3).

CD11c$^+$ APCs sorted from WT islets did not induce T-cell calcium fluxes and had a lower frequency of T cell–APC interactions (Fig. 3). In contrast, APCs sorted from antigen-containing early- (day 4.5) and late- (day 7) infiltrated islets showed equivalent abilities to induce T-cell interactions and calcium flux (Fig. 3). While participating in sustained interactions with T cells, islet APCs induced weak calcium signaling compared with the positive control (Fig. 3), likely due to low levels of endogenous antigen being presented (Fig. S4). Surprisingly, although islet-specific T cells differentially responded to CD11c$^+$ cells in the islets during early vs. late infiltration in vivo, we observed that the APCs from these two conditions were equally able to trigger T cells in vitro. Although this assay indicated that APCs from early- and late-infiltrated islets were equally able to present antigen to trigger T-cell signaling, the T-cell signaling could lead to either stimulation or tolerance.

Islet CD11c$^+$ Cells Cross-Present Islet Antigens to T Cells to Induce T Cell Receptor Signaling at the Disease Site. To directly determine whether the T cell–CD11c$^+$ cell interactions observed within the islets also induce T cell receptor (TCR) signaling, we used T cells from the OT-I–GFP mouse (19). This biosensor allows visualization of TCR dynamics in vivo, with TCR clustering and/or internalization reporting TCR signaling (19). During T cell–CD11c$^+$ cell interactions in the islets, we observed clear TCR clustering at the T cell–CD11c$^+$ cell interface (Fig. 4*A*). This TCR clustering shows that TCRs are engaging peptide–MHC complexes on CD11c$^+$ cells in the islets. Together, T-cell motility arrest on CD11c$^+$ APCs and TCR signaling detected with this biosensor demonstrate that islet CD11c$^+$ APCs serve to restimulate infiltrating T cells.

We then sought to understand the consequences of such T cell–APC engagements. Because OT-I T cells kill targets upon recognition, we asked whether these islet-infiltrating cytotoxic T lymphocytes were able to kill the CD11c$^+$ APCs that presented autoantigen to them (Fig. 4 *B* and *C* and Movie S4). We visualized lysis of APCs by the rapid loss of cytoplasmic fluorescence of CD11c-YFP$^+$ cells (Fig. 4*B*). Although relatively variable between islets, CD11c$^+$ cells died during interactions with T cells in 20% of interactions in islets with light infiltration, but CD11c$^+$ cell death was almost undetectable in islets with mid or heavy infiltration (Fig. 4*C*).

Environmental Cues in the Islet Regulate T-Cell Motility and Restimulation That Induces IFN-γ Production. The data thus far indicate an infiltration-dependent shift in interaction dynamics between T cells and APCs (Fig. 2), despite the fact that APCs from heavily infiltrated islets were still capable of delivering antigenic stimuli when tested ex vivo (Fig. 3). We therefore sought to determine whether the changes in T-cell motility and expression of T cell effector functions correlated with the state of islet infiltration or the duration of T-cell residence within the islet. To determine whether motility changes were dictated by environmental or T-cell intrinsic mechanisms, we transferred differentially marked OT-I T cells into RIP-mOva or WT hosts to track T cells that were in the same environment for different periods of time (Fig. 5*A*). On day 5 or 7 following transfer, corresponding to days in which light and midheavy infiltration

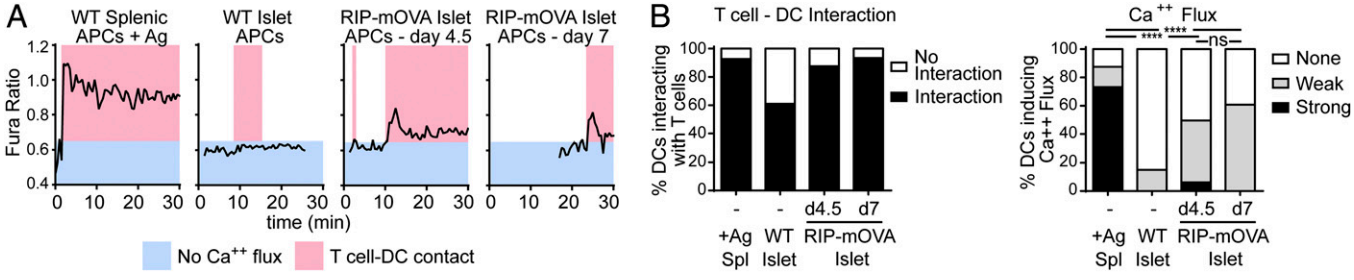

Fig. 3. CD11c$^+$ APCs in heavily infiltrated islets maintain the ability to trigger T cells. OT-I T cells were transferred into RIP-mOva recipients. Islets were isolated at different stages of infiltration: (–) no transfer control, (d4.5) early, (d7) late. CD11c$^+$MHCII^{hi}DAPI$^-$ APCs sorted from the spleen or islets were incubated with in vitro-activated OT-I T cells labeled with Fura-2AM. Splenic APCs were antigen-pulsed. T cell–APC interactions and Fura fluorescence were imaged by time-lapse widefield microscopy. Data combined from two experiments. $*P < 0.05$, $**P < 0.01$, $***P < 0.001$, $****P < 0.0001$. (*A*) Representative examples of calcium fluxes read out by Fura-2AM 340 nm/380 nm ratios. (*B*) Quantification of T cell–APC contacts and calcium-flux strength in T cells interacting with APCs. Statistics: Chi Square Test.

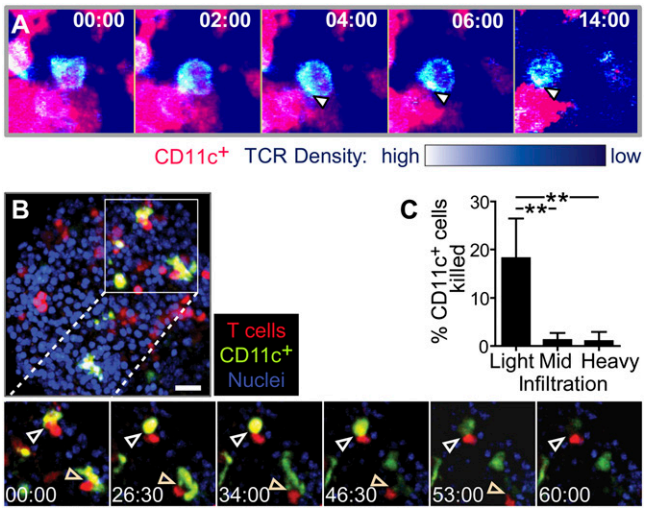

Fig. 4. Stable T cell–APC interactions induce TCR signaling and APC killing in the islets. (*A*) TCR central supramolecular activating complex (cSMAC) formation and internalization during interactions with CD11c$^+$ cells in the islets. OTI-TCR-GFP T cells were transferred into RIP-mOva.CD11c-mCherry recipients, and isolated islets were imaged by two-photon microscopy. TCR density is on a pseudocolor scale. Arrows indicate location of cSMAC, with internalized TCR visible in the last frame. Representative of two experiments. (*B* and *C*) APC killing by T cells in the islets. CD2-dsRed.OT-I T cells were transferred into RIP-mOva.CD11c-YFP recipients, and islets were imaged by two-photon microscopy. (*B*) Representative time-lapse of T cell-induced APC killing in a lightly infiltrated islet. Arrows indicate APC killing. Time-lapse represents 105 μm (x) × 105 μm (y) × 15 μm (z). Time stamp, min: sec. (*C*) Quantification of APC killing. Data combined from 10 experiments. $^{**}P < 0.01$ by 1-way ANOVA Kruskal–Wallis test with Dunn's Multiple Comparison Test.

was prevalent, islets from recipients designated for imaging experiments were harvested and analyzed by two-photon microscopy. Consistent with our previous analyses, we found a lower arrest coefficient in day 7-infiltrated islets versus day 5-infiltrated islets (Fig. 5*D*).

To determine whether this reduction in T-cell arrest resulted from a T cell-intrinsic change or a change in the islet environment, we performed serial T-cell transfers into the same recipients (Fig. 5*A*). If the differences were T cell-intrinsic, we would expect the T-cell populations transferred at different times to show differences in their motility despite a shared environment. If the differences resulted from environmental changes, we would expect the T cells transferred at different times to have similar behavior in the same environment. When islets had been infiltrated for 7 d, both populations of T cells behaved similarly; a low arrest coefficient was observed in the T cells that had been in mice for 5 d or 7 d (Fig. 5*D*). These results support a model in which T-APC dynamics were driven by the state of organ infiltration rather than the T-cell history.

The same conditions were used to analyze IFN-γ production as a readout of T cell effector function (Fig. 5*A*). Recipients for this analysis were treated in vivo with Brefeldin A to prevent cytokine secretion so it could be detected by intracellular cytokine staining. We found no significant IFN-γ production in draining or nondraining lymph nodes at the time points analyzed. However, on day 5 following T-cell transfer, there was significant IFN-γ production in the islets (Fig. 5 *B* and *C*), correlating with the day 4–5 time point when T-cell arrest and sustained interactions were seen (Figs. 1*E*, 2 *D* and *E*, and 5*D*). These data support the conclusion that the T-cell signaling observed in islets with light infiltration induces a restimulation event that leads to effector cytokine production.

A significant reduction in IFN-γ production was observed by day 7 following T-cell transfer (Fig. 5 *B* and *C*). This reduction in IFN-γ production correlated with an increase in T-cell motility and a decrease in T-cell arrest (Figs. 1 *D* and *E* and 5*D*). This correlation suggests that, in the absence of the restimulation occurring in arrested T cells, effector cytokine production was lost. Our results also showed diminished IFN-γ production and motility arrest 7 d posttransfer in both the early and late T-cell populations when tandem T-cell transfers were done. These results suggest that an environmental change induced increased T-cell motility and reduced T-cell arrest, leading to loss of effector cytokine production at the disease site (Fig. 5 *B* and *C*). A loss of CD25 expression on the transferred islet-specific T cells was also observed concomitant with the loss of T cell–APC interactions and IFN-γ production (Fig. 5*E*). Together, these data suggest that T-cell restimulation leading to effector cytokine production occurs during early-islet infiltration and is then lost due to environmental factors within the islet with increased infiltration.

CD11c$^+$ APC Populations Change with Islet Infiltration. Because our data showed a loss of T-cell interactions with CD11c$^+$ APCs and T cell effector function with increasing islet infiltration, we analyzed whether the CD11c$^+$ APC population changed with increasing infiltration. We found that recruitment of new populations of CD11c$^+$ APCs can be identified by CX3CR1 expression (Fig. 5 *F–H* and Fig. S5). In uninfiltrated islets, the resident CD11c$^+$ APCs were predominately CD11c$^+$CD11b$^+$ CX3CR1^{high}, with a small population of CD11c$^+$CD103$^+$ CX3CR1^{high} cells (Fig. 5 *F* and *H* and Fig. S5 *B* and *C*). Upon infiltration, local proliferation is insufficient to account for the increase in islet CD11c$^+$ APCs, suggesting APC recruitment (11). The resident CX3CR1^{high} APC populations remained with infiltration, and additional populations of CX3CR1^{low} cells were rapidly recruited to the islets with numbers that correlated with the degree of islet infiltration (Fig. 5 *G–H* and Fig. S5*B*). The recruited CX3CR1^{low} APCs were predominantly CD11b$^+$ but included some CD103$^+$ cells (Fig. S5*C*). Changes in the local functionality of resident versus recruited APCs may affect T-cell motility and interactions with increasing islet infiltration.

IFN-γ Production by Islet-Specific T Cells Is Required for Full Islet Infiltration and Disease Induction. IFN-γ production was lost as islet infiltration increased and T cell–CD11c+ cell interactions waned. IFN-γ production is suggested to be required for T-cell recruitment to the islets and disease acceleration (20, 21). To confirm that IFN-γ production affects this model, we analyzed T-cell infiltration of the islets and diabetes incidence (Fig. S6). We found a significant decrease in islet infiltration by IFN-γ–deficient T cells with no IFN-γ–dependent change in T-cell accumulation or expansion in draining or nondraining lymph nodes (Fig. S6*A*). Additionally, diabetes was not induced by IFN-γ–deficient T cells, compared with 30% diabetes incidence in mice that received WT T cells (Fig. S6*B*). Taken together, our data suggest that T-cell restimulation at the disease site is an integral part of the early phase of disease, being necessary both for effector cytokine production and for accelerated infiltration by T cells.

Discussion

The presented data demonstrate that T cell–APC interactions at the autoimmune disease site are modulated with disease progression and affect the effector state of autoreactive T cells. Our results show clear differences in T-cell behavior at the autoimmune disease site as islet infiltration and destruction progress. Using two-photon microscopy allowed us to investigate how progression of islet infiltration altered infiltrating T-cell behavior in situ within individual islets. The increased T-cell arrest and sustained T cell–APC interactions seen early in islet infiltration were associated with T cell effector cytokine production. On the other hand, as disease and tissue destruction progressed, T-cell motility increased and sustained interactions with APCs were lost, resulting in decreased effector cytokine production.

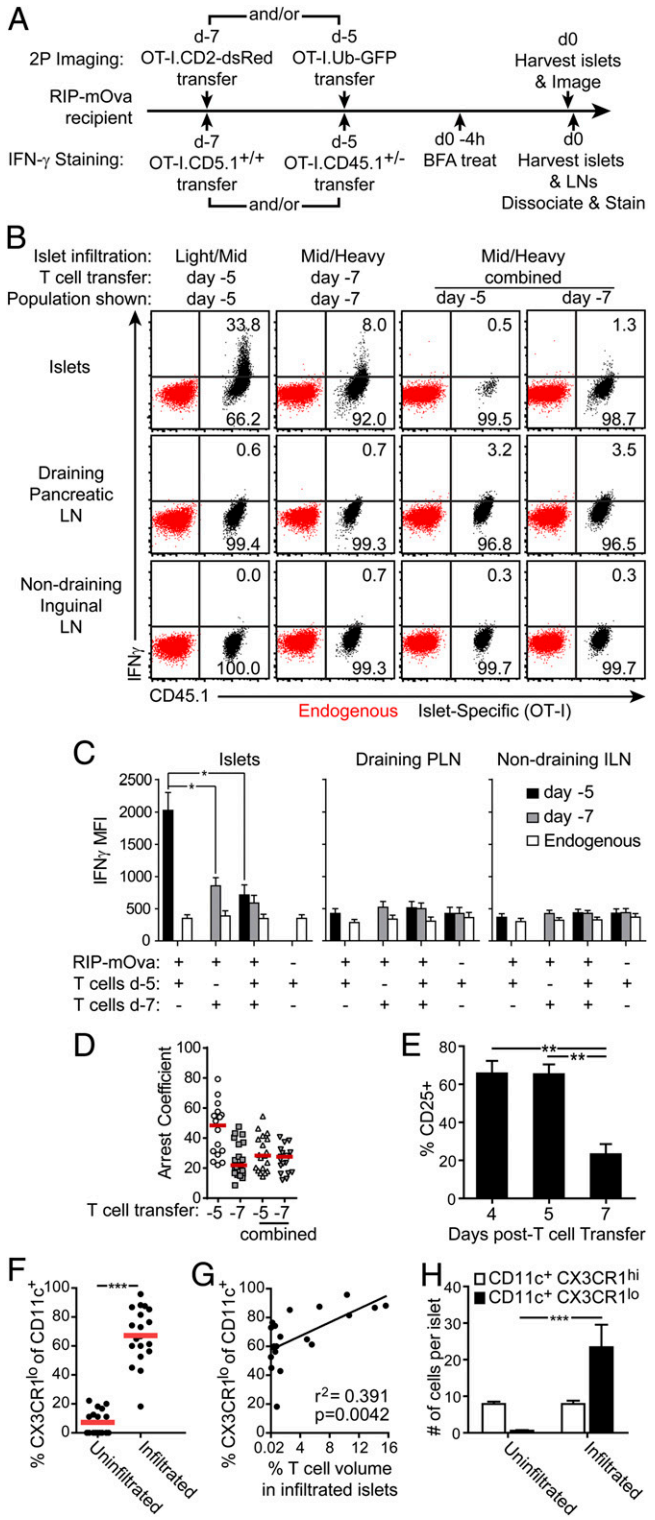

Fig. 5. T-cell dynamics and effector cytokine production are determined by the state of islet infiltration. (*A*) Experimental set-up for (*B–D*). (*B*) Induction of IFN-γ production in the islets is associated with T-cell arrest. Representative plots of in vivo IFN-γ production by intracellular cytokine staining. (*C*) Quantification of data shown in *B*. Data combined from six mice in three experiments. Statistics: 1-way ANOVA Kruskal–Wallis test with Dunn's Multiple Comparison Test. $*P < 0.05$. (*D*) Environmental factors prevent T-cell arrest in heavily infiltrated islets. Quantification of T-cell arrest coefficients analyzed by time-lapse two-photon imaging of T cells in early (d5) or late (d7) infiltrated islets. (*E*) CD25 expression is lost as T cells become more motile. Four animals per group combined from two experiments. $**P < 0.01$ by 1-way ANOVA Kruskal–Wallis test with Dunn's Multiple Comparison Test. (*F–H*) $CD11c^+CX3CR1^{low}$ APCs are recruited to the islets with infiltration. APC populations analyzed on a per-islet basis by two-photon microscopy at varying degrees of infiltration in RIP-mOva.CX3CR1-GFP.CD11c-YFP mice. Each dot represents one islet. (*F*) Uninfiltrated islets were analyzed in mice without T-cell transfer. $**P < 0.01$ by two-tailed *t* test. (*G*) Analysis of $CX3CR1^{low}$ APCs in infiltrated islets. $CX3CR1^{low}$ APCs correlate with T-cell infiltration. (*H*) Average cell count per islet of $CX3CR1^{low}$ versus $CX3CR1^{high}$ CD11c+ APCs with and without islet infiltration. $***P < 0.0001$ by 2-way ANOVA with Tukey's multiple comparison test.

Antigen presentation to T cells in the draining lymph nodes is critical for the initiation of autoimmunity. However, patients have established disease at diagnosis, so disrupting the initiation of disease is not a viable option. As a result, we chose to interrogate how antigen presentation and T-cell restimulation at the disease site promote and maintain the ongoing disease process. Our data suggest that, whereas T cells might be primed to produce effector cytokines such as IFN-γ during activation in the draining lymph node, they do not actually produce the effector cytokine until they are restimulated at the effector site. This obligate restimulation in the islet demonstrates a previously unidentified step in the progression of islet-specific autoimmunity and provides an important point of potential intervention when autoimmunity is already established.

Studies in the secondary lymphoid organs show that sustained interactions lead to T-cell activation whereas aborted or short-lived interactions result in tolerance (refs. 22–28, and reviewed in ref. 29). Although functional outcomes of T cell–APC interactions might be different in activated T cells in peripheral tissues, it is notable that we observed a reduced number of sustained interactions as infiltration progressed. One interpretation of these data is that we may be observing deletional tolerance as islet infiltration increases because the transfer of OT-I T cells in the RIP-mOva model eventually results in deletional tolerance. However, dying T cells arrest motility, and we observed increased T-cell motility in mid to heavy infiltrated islets, making it unlikely that these T cells were acutely dying. Additionally, in the NOD model, we see the same changes in CD4 T-cell motility with increased islet infiltration, suggesting that this progression is relevant in vastly different models of islet autoimmunity.

T cell–APC interactions have been suggested to promote entry into the autoimmune target tissue (4, 6) and effector cytokine production (4). On the other hand, in a mammary carcinoma tumor model, T cell–APC interactions at the disease site were associated with tolerance induction (30). Our data are consistent with findings, in a multiple sclerosis model (4), that suggest that T cell–APC interactions at the disease site can induce effector cytokine production. However, we further evaluated the role of these interactions as disease and tissue destruction progressed. Our resulting data show that, whereas effector cytokine is detectable in the presence of T cell–APC interactions at the disease site, it is temporally confined to the early-infiltration phase and is lost in highly infiltrated tissues, concurrent with the loss of stable T cell–APC interactions. This effect is at least partially dependent upon conditioning of the islet environment.

There are a variety of environmental and cell-intrinsic factors that could be contributing to the loss of sustained T cell–APC interactions. Reduced T-cell stopping and APC interactions do not appear to be dependent on the ability of the islet APCs to present antigen. However, we show that the population of islet APCs evolves as islet infiltration progresses (11). Thus, the changes in T cell–APC interactions likely depend at least in part upon the subset and phenotype of the APCs. Loss of antigen-specific T cell–APC interactions in the draining lymph node in T1D can be a result of antigen-specific regulatory T-cell activity (25) or due to PD-1–PD-L1 interactions (27). A variety of inhibitory receptor-ligand pairs, including but not limited to PD-1–PD-L1/PD-L2, CTLA-4–CD80/CD86, and LAG-3–MHC class

IMMUNOLOGY

II, could be influencing the ability of T cells to recognize their antigen in the islets (27, 31–33). Our data suggest that these checkpoint receptors are not mediating the changes in the dynamics of T-cell restimulation. A variety of chemokines are up-regulated in the islet environment in response to infiltration (34) that could influence T-cell sensitivity to antigen receptor signaling (35, 36). It is likely that the loss of T cell–APC interactions seen in our experiments may be a result of several mechanisms.

Using two-photon microscopy of individual islets at different stages of disease has allowed us to identify how the behavior of T cells is altered between islets within the same animal depending upon the stage of infiltration. Because islet infiltration is an asynchronous process, it is important to recognize that the disease processes occurring within an individual pancreas differ from islet to islet. As a result, interventions might differentially affect individual islets depending upon their infiltration state. This approach allows us to evaluate the dynamic nature of disease progression within individual islets and assess how interventions affect islets at different stages of disease. Here, we have identified a restimulation event in the islets that leads to effector cytokine production. This restimulation step provides a potential node of intervention for preventing progression of islet infiltration and destruction.

Materials and Methods

See *SI Materials and Methods* for details.

Mice. The experimental procedures were approved subject to, and mice were handled in accordance with, the guidelines of the University of California, San Francisco and the National Jewish Health Institutional Animal Care and Use Committee.

Two-Photon in Situ Islet Imaging and Analysis. Islet isolation was done as described (11). During imaging, islets were maintained at 35–37 °C in media saturated with 95% O_2/5% CO_2. Two-photon imaging was done using a custom-built instrument (37) or a four-channel Olympus FV1000MPE microscope (38). Data were analyzed using Imaris (Bitplane) and MATLAB (Mathworks).

Detection of in Vivo IFN-γ Production. For detection of in vivo IFN-γ production, mice were treated with 10 μg/g body weight Brefeldin A (Sigma Aldrich) injected i.v. 4–6 h before harvest. Islets were dissociated with a nonenzymatic cell dissociation solution (Sigma-Aldrich), blocked, and stained for flow cytometry.

Calcium Imaging. $CD11c^+$ MHC class II^{hi} $DAPI^-$ cells were sorted from spleen or islets. Sorted $CD11c^+$ cells were plated in fibronectin-coated wells with Fura-2AM–labeled, in vitro-activated OT-I T cells. Calcium flux was determined based on the ratio of Fura fluorescence at 340 nm/380 nm.

ACKNOWLEDGMENTS. We thank Pete Beemiller and Bonnie Leavitt for programming of image-analysis scripts, Eric Wigton for animal-colony maintenance, and Audrey Gerard and Jenny Kemp for critical reading of the manuscript. This work was funded by the Larry L. Hillblom Foundation (R.S.F.), National Jewish Health (R.S.F.), JDRF Grants 1-2007-170 (to M.F.K.) and 2-2012-197 (to R.S.F.), and Cancer Research Institute Training Grant 63003254 (to R.S.L.).

1. Wakim LM, Waithman J, van Rooijen N, Heath WR, Carbone FR (2008) Dendritic cell-induced memory T cell activation in nonlymphoid tissues. *Science* 319(5860):198–202.
2. Hufford MM, Kim TS, Sun J, Braciale TJ (2011) Antiviral $CD8^+$ T cell effector activities in situ are regulated by target cell type. *J Exp Med* 208(1):167–180.
3. McLachlan JB, Catron DM, Moon JJ, Jenkins MK (2009) Dendritic cell antigen presentation drives simultaneous cytokine production by effector and regulatory T cells in inflamed skin. *Immunity* 30(2):277–288.
4. Bartholomäus I, et al. (2009) Effector T cell interactions with meningeal vascular structures in nascent autoimmune CNS lesions. *Nature* 462(7269):94–98.
5. Graham KL, et al. (2011) Autoreactive cytotoxic T lymphocytes acquire higher expression of cytotoxic effector markers in the islets of NOD mice after priming in pancreatic lymph nodes. *Am J Pathol* 178(6):2716–2725.
6. Calderon B, Carrero JA, Miller MJ, Unanue ER (2011) Cellular and molecular events in the localization of diabetogenic T cells to islets of Langerhans. *Proc Natl Acad Sci USA* 108(4):1561–1566.
7. Gagnerault MC, Luan JJ, Lotton C, Lepault F (2002) Pancreatic lymph nodes are required for priming of beta cell reactive T cells in NOD mice. *J Exp Med* 196(3):369–377.
8. Turley S, Poirot L, Hattori M, Benoist C, Mathis D (2003) Physiological beta cell death triggers priming of self-reactive T cells by dendritic cells in a type-1 diabetes model. *J Exp Med* 198(10):1527–1537.
9. Levisetti MG, Suri A, Frederick K, Unanue ER (2004) Absence of lymph nodes in NOD mice treated with lymphotoxin-beta receptor immunoglobulin protects from diabetes. *Diabetes* 53(12):3115–3119.
10. Saxena V, Ondr JK, Magnusen AF, Munn DH, Katz JD (2007) The countervailing actions of myeloid and plasmacytoid dendritic cells control autoimmune diabetes in the nonobese diabetic mouse. *J Immunol* 179(8):5041–5053.
11. Melli K, et al. (2009) Amplification of autoimmune response through induction of dendritic cell maturation in inflamed tissues. *J Immunol* 182(5):2590–2600.
12. Calderon B, Suri A, Miller MJ, Unanue ER (2008) Dendritic cells in islets of Langerhans constitutively present beta cell-derived peptides bound to their class II MHC molecules. *Proc Natl Acad Sci USA* 105(16):6121–6126.
13. Yin N, et al. (2012) Functional specialization of islet dendritic cell subsets. *J Immunol* 188(10):4921–4930.
14. Kurts C, et al. (1996) Constitutive class I-restricted exogenous presentation of self antigens in vivo. *J Exp Med* 184(3):923–930.
15. Kurts C, et al. (1997) CD4+ T cell help impairs CD8+ T cell deletion induced by cross-presentation of self-antigens and favors autoimmunity. *J Exp Med* 186(12): 2057–2062.
16. Veiga-Fernandes H, et al. (2007) Tyrosine kinase receptor RET is a key regulator of Peyer's patch organogenesis. *Nature* 446(7135):547–551.
17. Lindquist RL, et al. (2004) Visualizing dendritic cell networks in vivo. *Nat Immunol* 5(12):1243–1250.
18. Coppieters K, Amirian N, von Herrath M (2012) Intravital imaging of CTLs killing islet cells in diabetic mice. *J Clin Invest* 122(1):119–131.
19. Friedman RS, Beemiller P, Sorensen CM, Jacobelli J, Krummel MF (2010) Real-time analysis of T cell receptors in naive cells in vitro and in vivo reveals flexibility in synapse and signaling dynamics. *J Exp Med* 207(12):2733–2749.
20. Calderon B, Carrero JA, Miller MJ, Unanue ER (2011) Entry of diabetogenic T cells into islets induces changes that lead to amplification of the cellular response. *Proc Natl Acad Sci USA* 108(4):1567–1572.
21. Savinov AY, Wong FS, Chervonsky AV (2001) IFN-gamma affects homing of diabetogenic T cells. *J Immunol* 167(11):6637–6643.
22. Hugues S, et al. (2004) Distinct T cell dynamics in lymph nodes during the induction of tolerance and immunity. *Nat Immunol* 5(12):1235–1242.
23. Zinselmeyer BH, et al. (2005) In situ characterization of CD4+ T cell behavior in mucosal and systemic lymphoid tissues during the induction of oral priming and tolerance. *J Exp Med* 201(11):1815–1823.
24. Shakhar G, et al. (2005) Stable T cell-dendritic cell interactions precede the development of both tolerance and immunity in vivo. *Nat Immunol* 6(7):707–714.
25. Tang Q, et al. (2006) Visualizing regulatory T cell control of autoimmune responses in nonobese diabetic mice. *Nat Immunol* 7(1):83–92.
26. Tadokoro CE, et al. (2006) Regulatory T cells inhibit stable contacts between CD4+ T cells and dendritic cells in vivo. *J Exp Med* 203(3):505–511.
27. Fife BT, et al. (2009) Interactions between PD-1 and PD-L1 promote tolerance by blocking the TCR-induced stop signal. *Nat Immunol* 10(11):1185–1192.
28. Katzman SD, et al. (2010) Duration of antigen receptor signaling determines T-cell tolerance or activation. *Proc Natl Acad Sci USA* 107(42):18085–18090.
29. Jacobelli J, Lindsay RS, Friedman RS (2013) Peripheral tolerance and autoimmunity: lessons from in vivo imaging. *Immunol Res* 55(1-3):146–154.
30. Engelhardt JJ, et al. (2012) Marginating dendritic cells of the tumor microenvironment cross-present tumor antigens and stably engage tumor-specific T cells. *Cancer Cell* 21(3):402–417.
31. Okazaki T, et al. (2011) PD-1 and LAG-3 inhibitory co-receptors act synergistically to prevent autoimmunity in mice. *J Exp Med* 208(2):395–407.
32. Lu Y, Schneider H, Rudd CE (2012) Murine regulatory T cells differ from conventional T cells in resisting the CTLA-4 reversal of TCR stop-signal. *Blood* 120(23):4560–4570.
33. Bettini M, et al. (2011) Cutting edge: Accelerated autoimmune diabetes in the absence of LAG-3. *J Immunol* 187(7):3493–3498.
34. Sarkar SA, et al. (2012) Expression and regulation of chemokines in murine and human type 1 diabetes. *Diabetes* 61(2):436–446.
35. Friedman RS, Jacobelli J, Krummel MF (2006) Surface-bound chemokines capture and prime T cells for synapse formation. *Nat Immunol* 7(10):1101–1108.
36. Bromley SK, Peterson DA, Gunn MD, Dustin ML (2000) Cutting edge: Hierarchy of chemokine receptor and TCR signals regulating T cell migration and proliferation. *J Immunol* 165(1):15–19.
37. Bullen A, Friedman RS, Krummel MF (2009) Two-photon imaging of the immune system: A custom technology platform for high-speed, multi-color tissue imaging of immune responses. *Curr Top Microbiol Immunol* 334:1-29.
38. McKee AS, et al. (2013) Host DNA released in response to aluminum adjuvant enhances MHC class II-mediated antigen presentation and prolongs CD4 T-cell interactions with dendritic cells. *Proc Natl Acad Sci USA* 110(12):E1122–E1131.